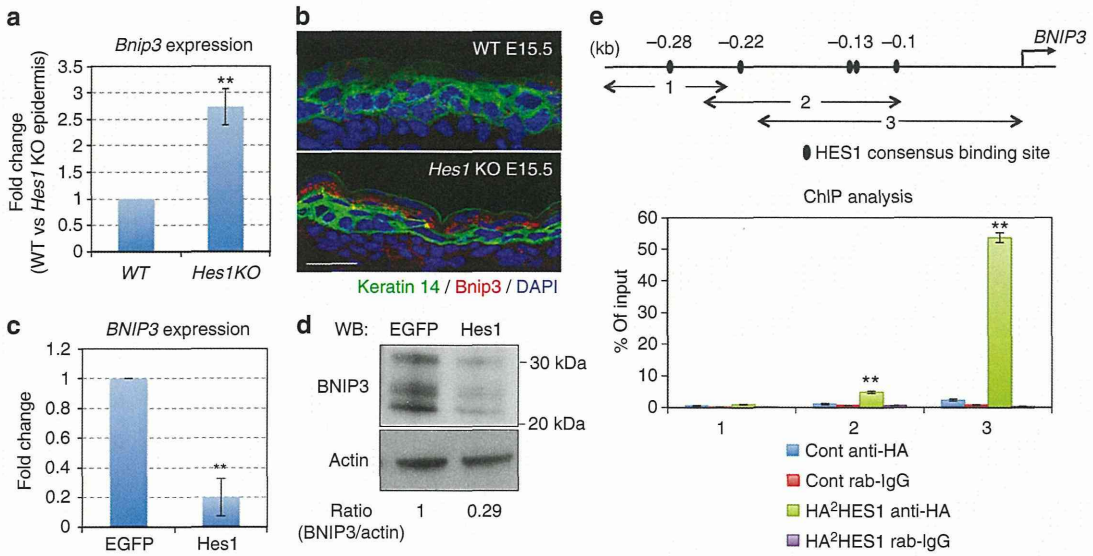

Figure 1. BNIP3 (BCL2 and adenovirus E1B 19-kDa-interacting protein 3) is directly suppressed by HES1(hairy and enhancer of split-1). (**a**) Quantitative PCR (Q-PCR) analysis of *Bnip3* expression in dorsal skin epidermis from either wild-type (WT) or *Hes1* knockout (KO) embryo (embryonic day 14.5 (E14.5)). (**b**) Immunofluorescent analysis of Bnip3 expression in dorsal skin epidermis from either WT or *Hes1* KO embryo (E15.5). Keratin 14 staining is shown in green and Bnip3 staining is shown in red. The blue signals indicate nuclear staining. Scale bars = 20 μm. (**c**) Q-PCR and (**d**) western blot analysis of BNIP3 expression in human primary epidermal keratinocyte (HPEK) cells infected with adenoviruses expressing enhanced green fluorescent protein (EGFP) or Hes1. (**c**) Each expression value was calculated with the ΔΔCt method using *UBE2D2* as an internal control. (**d**) Numbers below blots indicate relative band intensities as determined by ImageJ software. (**e**) Specific binding of Hes1 to the *BNIP3* promoter. HPEK cells were infected with adenoviral constructs expressing hemagglutinin (HA)-tagged Hes1, and processed for chromatin immunoprecipitation (ChIP) with an anti-HA antibody and normal rabbit immunoglobulin G (Cont rab-IgG) as a nonimmune control. Q-PCR amplification of the region of the *BNIP3* gene described in the indicated map (upper panel; nucleotides −360 to −244 (1); nucleotides −247 to −87 (2); −212 to +22 (3)) was also performed. The amount of precipitated DNA was calculated relative to the total input chromatin. All the data represent the average of three independent experiments ± SD. $^{**}P<0.01$.

with a BNIP3 adenoviral vector. BNIP3 expression was found to be sufficient to trigger the formation of EGFP-LC3 puncta that was significantly reduced by addition of 3-methyladenine (3-MA), an inhibitor of autophagy (Figure 3a and b). On the other hand, BNIP3 knockdown markedly decreased the punctuate distribution of EGFP-LC3 in differentiated HPEKs (Figure 3c and d). Furthermore, flow cytometry analysis using a green fluorescent probe used to specifically detect autophagy (Cyto-ID autophagy detection dye) (Chan *et al.*, 2012) also showed that BNIP3 was required for the autophagy induction (Figure 3c and f). These data indicate that BNIP3 is involved in the induction of autophagy in HPEKs. Intriguingly, these data also confirm the previous finding that autophagosome induction is accompanied by keratinocyte differentiation (Haruna *et al.*, 2008). We observed that the number of mitochondria was decreased in the granular layers, where BNIP3 expression and autophagosome formation was observed (Figure 4a). In addition, mitochondria were significantly decreased in the differentiated HPEKs *in vitro* (Figure 4b). Colocalizations of mitochondria and EGFP-LC3 dot were observed only in the differentiating keratinocytes (Figure 4c), suggesting the contribution of autophagy in the decrease of mitochondria. BNIP3 expression was also correlated with decreased mitochondria in HPEKs, whereas addition of 3-MA restored mitochondrial numbers (Figure 4d). Furthermore, we also observed colocalization of mitochondria and EGFP-LC3 dot in BNIP3-overexpressing HPEKs (Figure 4e). These data indicated that mitochondria were removed by BNIP3-induced autophagy. Next, we investigated the involvement of BNIP3 in the differentiation of epidermal keratinocytes. Western blot analysis and immunofluorescent staining revealed that BNIP3 expression increased during differentiation (Figure 5a and b). Knockdown of BNIP3 significantly suppressed keratinocyte differentiation when the cells were treated with differentiation medium (Figure 5c and d), indicating that BNIP3 is required for terminal differentiation of keratinocyte. On the other hand, forced expression of BNIP3 in HPEKs markedly stimulated loricrin expression (Figure 5e and f). To determine whether BNIP3-dependent keratinocyte differentiation was induced by autophagy, 3-MA was added to the cells transduced with BNIP3. As shown in Figure 5e and f, 3-MA notably abolished the keratinocyte differentiation induced by BNIP3, suggesting that BNIP3 is required for terminal differentiation of keratinocyte by induction of autophagy.

BNIP3 maintains epidermal keratinocytes

To further determine the roles of BNIP3 in epidermal differentiation, the human skin epidermal equivalent was reconstituted from HPEKs stably expressing a BNIP3 RNA interference (RNAi). Unfortunately, we did not observe drastic differentiation defects; however, we unexpectedly discovered

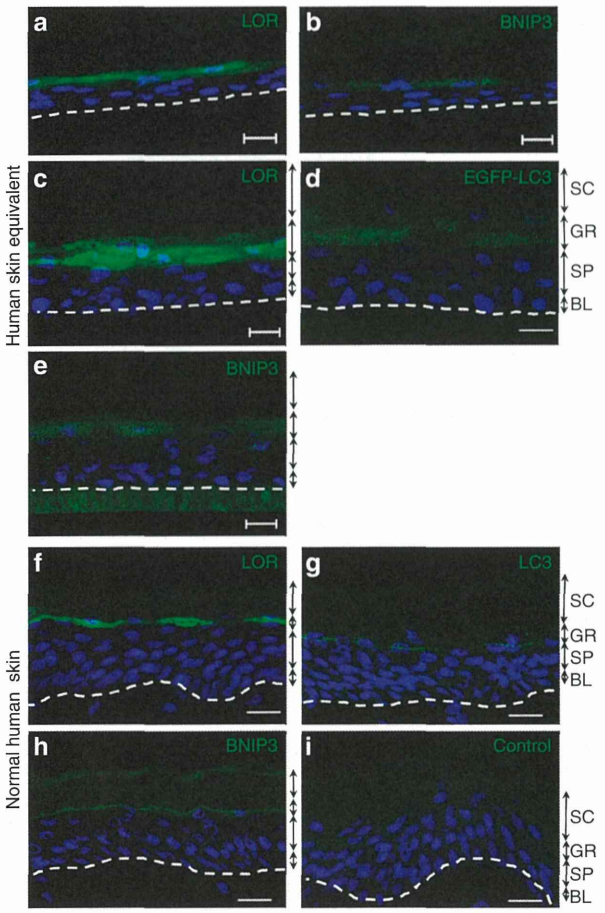

Figure 2. BNIP3 (BCL2 and adenovirus E1B 19-kDa-interacting protein 3) is expressed in the granular layer of the human epidermis. (**a**–**e**) Human skin epidermal equivalents were constituted from (**a**–**d**) normal human primary epidermal keratinocytes (HPEKs) or (**e**) HPEKs transfected with EGFP-LC3 by lentiviral vector. Cells were grown for (**a**, **b**) 18 days and (**c**–**e**) 24 days after exposure at the air–liquid interface. (**f**–**i**) Normal human skin epidermis. (**a**, **c**, **f**) Expression pattern of loricrin (LOR). (**b**, **e**, **h**) Expression pattern of BNIP3. (**i**) Control staining without BNIP3 antibody is shown. (**d**) Autophagosome formation determined by EGFP-LC3 puncta. (**g**) Endogenous expression pattern of LC3. The blue signals indicate nuclear staining. The dotted lines indicate (**a**–**e**) the boundary between the epidermis and the membrane or (**f**–**i**) the boundary between the epidermis and the dermis. Scale bars = 20 μm. BL, basal layer; GL, granular layer; SC, stratum corneum (cornified layer); SP, spinous layer.

that "sunburn-like cells" existed in BNIP3 knockdown epidermal equivalent (Figure 6a and b). We therefore hypothesized that BNIP3 might play a key role in the survival of epidermal keratinocytes. To evaluate this hypothesis, HPEKs were irradiated with 20 mJ cm^{-2} UVB. UVB irradiation triggered the formation of autophagosome that was significantly reduced by BNIP3 knockdown (Figure 6c–e). As shown in Figure 6f, UVB irradiation induced cleavage of caspase3 and BNIP3 expression. Intriguingly, knockdown of UVB-induced BNIP3 by RNAi further increased the amount of cleaved caspase3, suggesting that BNIP3 is required for the protection of keratinocytes from UVB-induced apoptosis (Figure 6f).

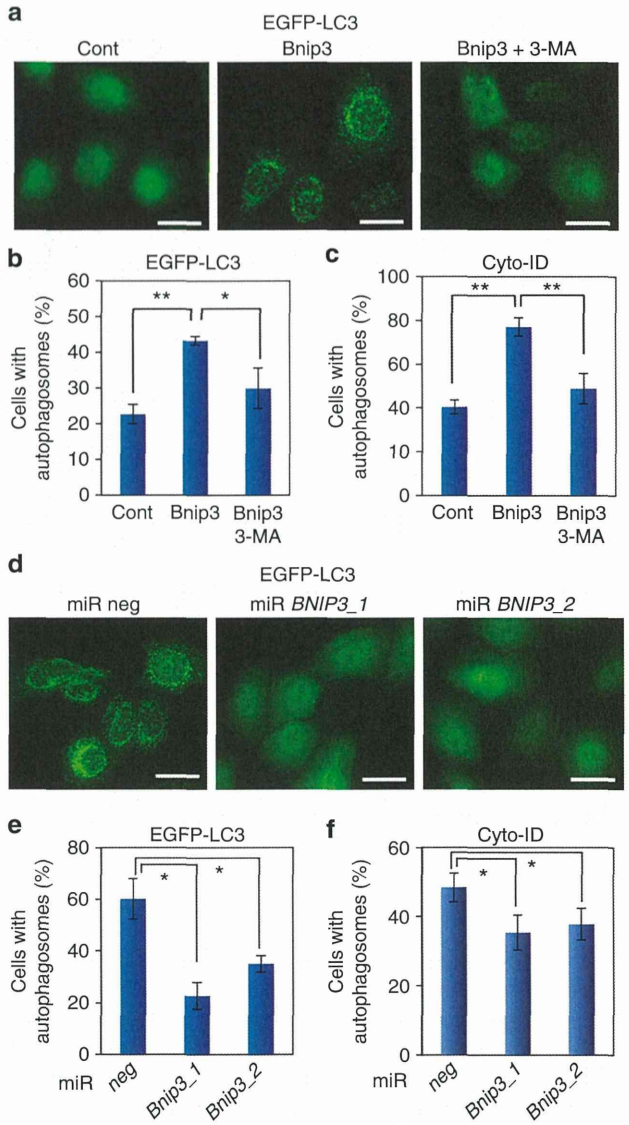

Figure 3. BNIP3 (BCL2 and adenovirus E1B 19-kDa-interacting protein 3) stimulates autophagy. (**a**, **b**) EGFP-LC3-expressing human primary epidermal keratinocytes (HPEKs) were transduced with DsRed (Cont) or BNIP3. As an inhibitor of autophagy, 3-methyladenine 3-MA (5 mM) was added. Cells were then stained with anti-EGFP at 24 hours after transduction. (**a**) EGFP-LC3 staining is shown in green. Scale bars = 20 μm. (**b**) The percentage of EGFP-LC3-positive cells with more than five puncta were quantified and are presented as the mean of three independent experiments ± SD. (**c**) HPEKs were transduced with DsRed (Cont) or BNIP3. As an inhibitor of autophagy, 3-MA (5 mM) was added. Autophagy induction was determined by Cyto-ID staining and quantified by flow cytometry. (**d**, **e**) EGFP-LC3-expressing HPEKs were transduced with miR *neg*, miR *BNIP3_1*, or miR *BNIP3_2* and induced to differentiate. Cells were then stained with anti-EGFP at 8 hours after differentiation induction. (**d**) EGFP-LC3 staining is shown in green. Scale bars = 20 μm. (**e**) The percentage of EGFP-LC3-positive cells with more than five puncta were quantified and are presented as the mean of three independent experiments ± SD. (**f**) HPEKs were transduced with miR *neg*, miR *BNIP3_1*, or miR *BNIP3_2* and induced to differentiate. Autophagy induction was determined by Cyto-ID staining and quantified by flow cytometry. All the data represent the average of three independent experiments ± SD. $^{**}P<0.01$; $^{*}0.01<P<0.05$.

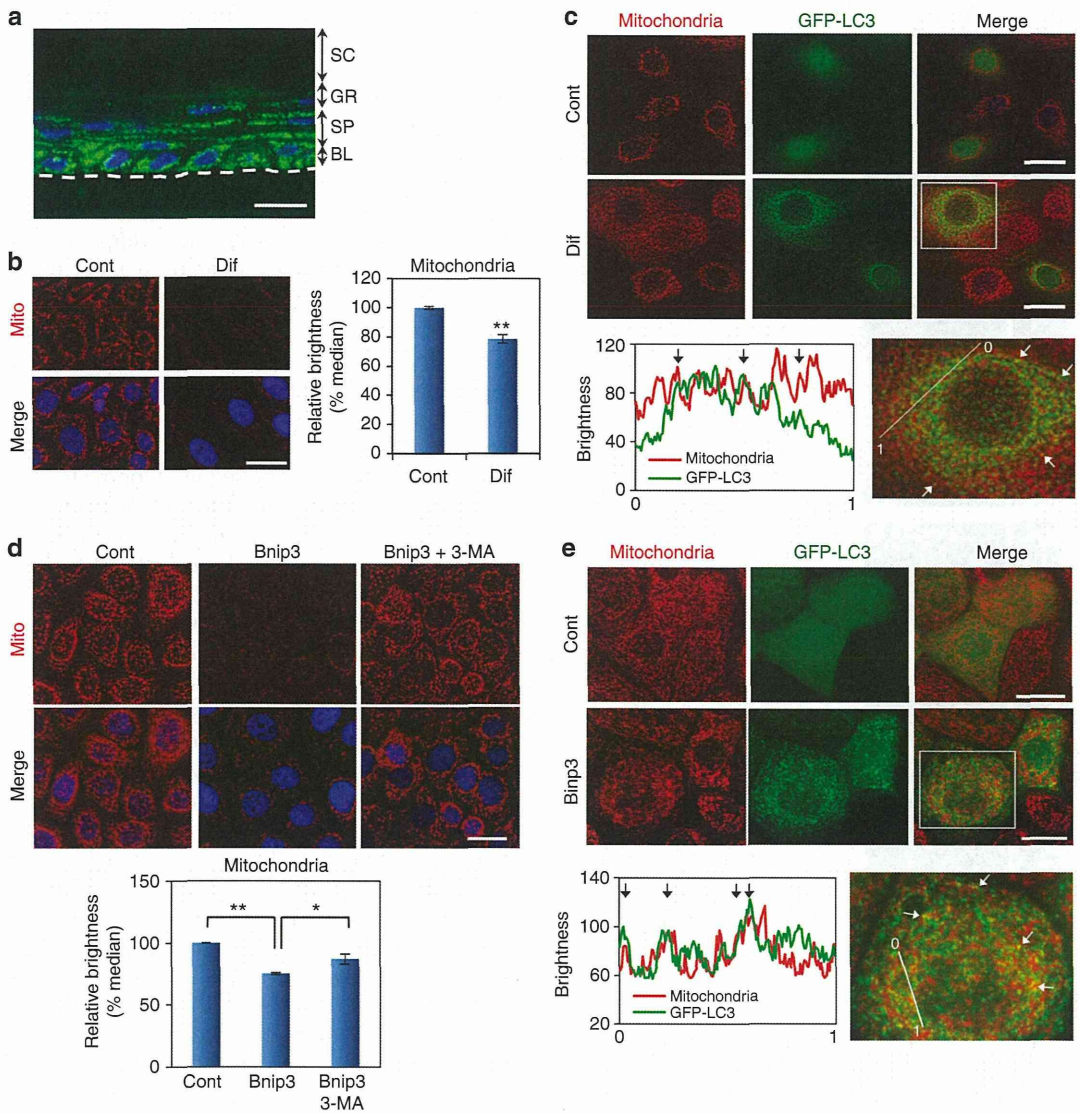

Figure 4. Autophagy stimulates mitochondrial degradation. (**a**) Distribution pattern of mitochondria. The blue signals indicate nuclear staining. The dotted lines indicate the boundary between the epidermis and the membrane. Scale bars = 20 μm. BL, basal layer; GL, granular layer; SC, stratum corneum (cornified layer); SP, spinous layer. (**b**) Nondifferentiated control (Cont) or differentiated human primary epidermal keratinocytes (HPEKs; Dif) were subjected to immunofluorescent staining 2 days after induction of differentiation. Mitochondrial staining is shown in red. The blue signals indicate nuclear staining. Scale bar = 20 μm. The graph indicates the percent of median brightness calculated by BZ Analyzer Software (Keyence) as the mean of three independent experiments ± SD. (**c**) EGFP-LC3-expressing HPEKs were differentiated. Cont or Dif were stained with anti-mitochondria (red) and anti-EGFP (green) 8 hours after induction of differentiation. Graph indicates the linescan analysis of the red and green fluorescent channels. Initial point of linescan is indicated as 0, and terminal point is indicated as 1. The arrows mark the colocalization of the two proteins. (**d**) HPEKs were transduced with enhanced green fluorescent protein (EGFP; Cont) or BNIP3 (BCL2 and adenovirus E1B 19-kDa-interacting protein 3). As an inhibitor of autophagy, 3-methyladenine 3-MA (5 mM) was added. Cells were then fixed and stained with anti-mitochondria 48 hours after transduction. Scale bar = 20 μm. The graph indicates the percent of median brightness calculated by BZ Analyzer Software (Keyence) as the mean of three independent experiments. $^{**}P<0.01$; $^{*}0.01<P<0.05$. (**e**) EGFP-LC3-expressing HPEKs were transduced with mock (Cont) or BNIP3. Cells were then fixed and stained with anti-mitochondria (red) and anti-EGFP (green) 24 hours after transduction. Graph indicates the linescan analysis of the red and green fluorescent channels. Initial point of linescan is indicated as 0, and terminal point is indicated as 1. The arrows mark the colocalization of the two proteins.

DISCUSSION

In this study, we demonstrated that BNIP3, a potent inducer of autophagy, plays a role in the terminal differentiation and maintenance of epidermal keratinocytes. It has been suggested that autophagy plays a role in the skin epidermis, but few attempts have been made to clarify the involvement of autophagy in skin epidermis.

We found that the HES1 transcriptional repressor directly suppressed BNIP3 expression in mouse epidermis and HPEKs (Figure 1). Moreover, our results revealed that BNIP3 was

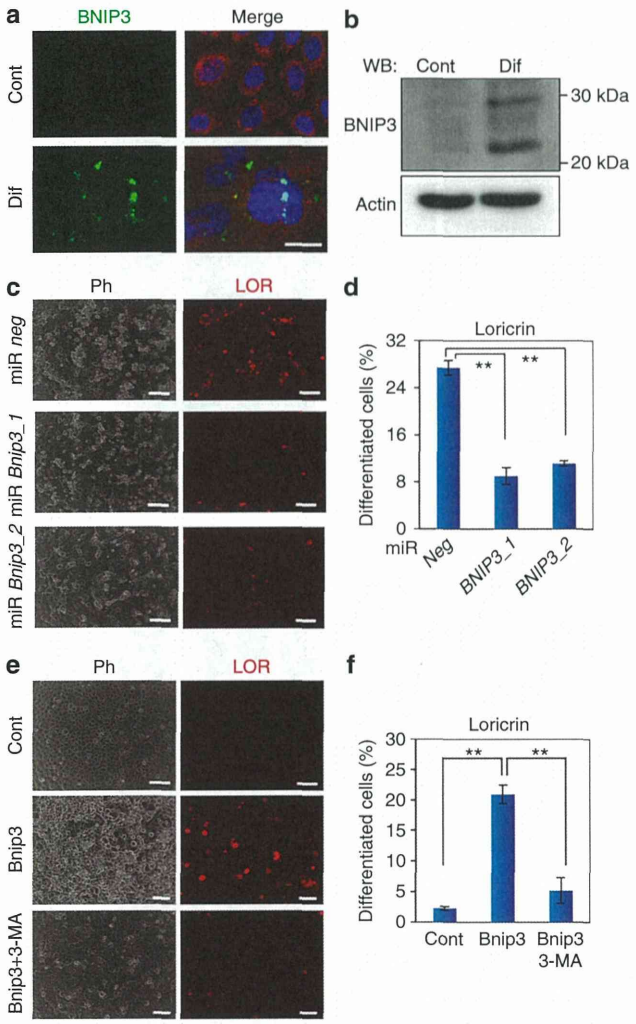

Figure 5. BNIP3 (BCL2 and adenovirus E1B 19-kDa-interacting protein 3) is required for the differentiation of keratinocytes *in vitro*. (**a**, **b**) Human primary epidermal keratinocytes (HPEKs) were differentiated and BNIP3 expression was observed. (**a**) Nondifferentiated control (Cont) or differentiated HPEKs (Dif) were subjected to immunofluorescent staining. BNIP3 staining is shown in green. Mitochondrial staining is shown in red. The blue signals indicate nuclear staining. Scale bar = 20 μm. (**b**) Western blot (WB) analysis. Proteins extracted from Cont or Dif were probed with anti-BNIP3 or anti-actin. (**c**, **d**) HPEKs were infected with adenoviral vectors expressing miR *neg*, miR *BNIP3_1*, or miR *BNIP3_2* followed by induction of differentiation. Cells were then immunostained with a loricrin antibody 9 days after transduction. (**e**, **f**) HPEKs were infected with adenoviral vectors expressing enhanced green fluorescent protein (EGFP; Cont) or BNIP3 and subjected to immunofluorescent staining against loricrin (LOR) 6 days after transduction. As an inhibitor of autophagy, 3-methyladenine 3-MA (5 mM) was added. Phase contrast images (Ph) and LOR staining are shown. Scale bars = 200 μm. (**d**, **f**) Percentages of LOR-positive differentiated cells were calculated by computerized image analysis. The data represent the average of three independent experiments ± SD. $^{**}P<0.01$.

expressed in the granular layers of mouse epidermis, its human skin epidermal equivalent, and its normal human skin epidermis (Figures 1 and 2). These data are consistent with our previous report showing that Hes1 is expressed in the spinous layers, where it represses the regulatory genes for differentiation to maintain the spinous cell fate (Moriyama *et al.*, 2008). Hence, it can be inferred that Bnip3 expression is suppressed in the spinous layers by Hes1, whereas it is upregulated in the granular layers where Hes1 expression is absent. In addition, our finding that BNIP3 is required for keratinocyte differentiation fits our idea that Hes1 represses certain regulatory genes to prevent the premature differentiation of spinous cells. Our *in vitro* data suggest that BNIP3 is involved in keratinocyte differentiation through autophagy (Figures 3–5). The mechanisms underlying the involvement of autophagy in keratinocyte differentiation remain elusive; however, considering that keratinocyte differentiation induced mitochondrial clearance and BNIP3 expression (Figure 4 and 5), BNIP3-induced autophagy may be responsible for the removal of mitochondria that may be required for the terminal differentiation of epidermal keratinocytes. During reticulocyte differentiation, programmed clearance of mitochondria induced by BNIP3L/Nix, a molecule closely related to BNIP3, has been reported to be a critical step (Schweers *et al.*, 2007). Therefore, keratinocytes likely possess the same differentiation mechanism that reticulocytes have, although further investigation will be required for elucidation.

In contrast to the results from differentiation in two-dimensional culture, we did not observe drastic differentiation defects in the BNIP3 knockdown human epidermal equivalent except for the existence of "sunburn-like cells" (Figure 6). This might be because of the incomplete suppression of BNIP3 in the BNIP3 knockdown keratinocytes, and/or might be because of the redundancy between BNIP3 and BNIP3L/Nix, a homolog of BNIP3, as we found in our preliminary study that Bnip3l is also expressed in the epidermis (data not shown). Although the phenotypes of BNIP3-null mice were published in 2007, these researchers found that BNIP3-null mice had no increase in mortality or apparent physical abnormalities (Diwan *et al.*, 2007). Generally, impairment of epidermal differentiation or skin barrier formation results in an obvious defect. Thus, BNIP3-null epidermis seems to exhibit subtle, if any, abnormalities. On the basis of these findings, the involvement of BNIP3 in epidermal differentiation must be investigated in the future. In-depth analysis of the BNIP3-null epidermis phenotype could help elucidate the role of BNIP3 in mouse epidermal differentiation.

Despite the lack of obvious differentiation defects in the human epidermal equivalent, our data showing that BNIP3 knockdown caused the appearance of "sunburn-like cells" is regarded as an example of apoptosis (Young, 1987), revealing a new role of BNIP3 in keratinocyte maintenance. Furthermore, requirement of BNIP3 for protection from UV-induced apoptosis was confirmed in two-dimensional keratinocyte cultures (Figure 6e). The underlying mechanism of this prosurvival function of BNIP3 in keratinocytes remains unclear; however, previous reports have demonstrated that hypoxia-induced autophagy through BNIP3 is critical for the prosurvival process (Bellot *et al.*, 2009). Recently, it has been reported that UVA induces autophagy to remove oxidized phospholipids and protein aggregates in epidermal keratino-

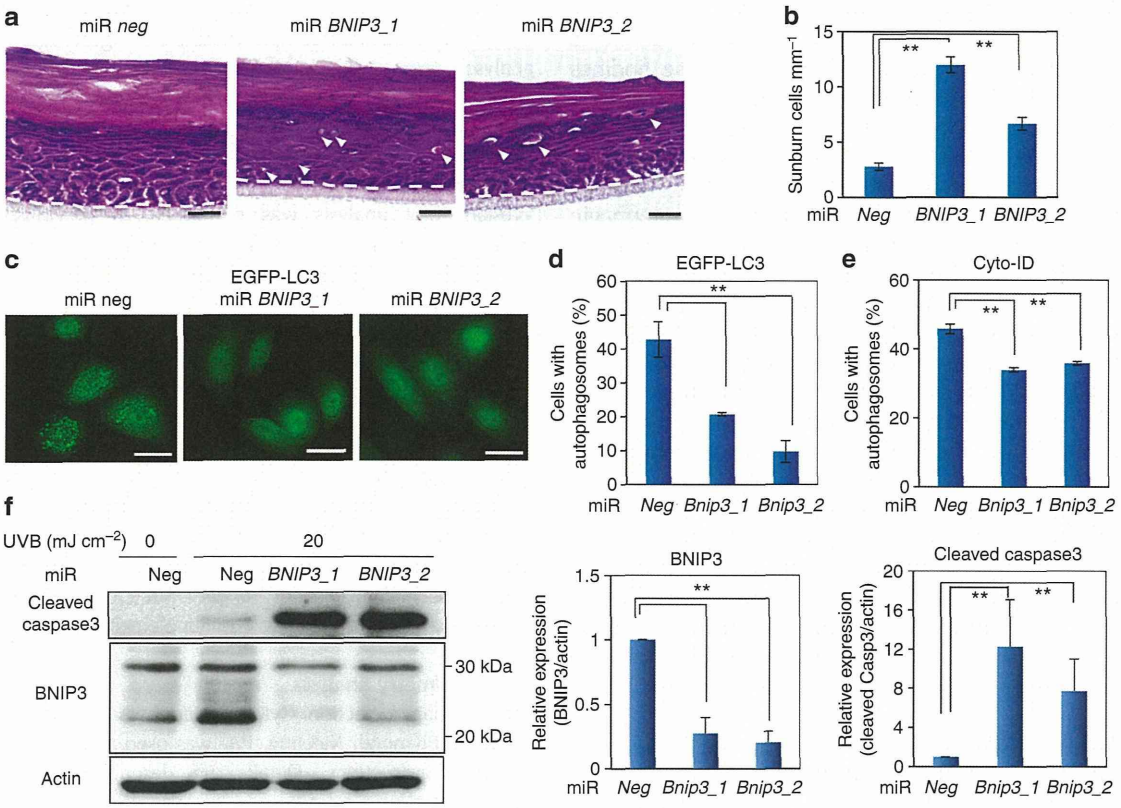

Figure 6. BNIP3 (BCL2 and adenovirus E1B 19-kDa-interacting protein 3) promotes cell survival in the reconstituted epidermis and keratinocytes. (**a**) Morphology of the human skin epidermal equivalents from human primary epidermal keratinocytes (HPEKs) infected with lentivirus expressing miR *neg*, miR *BNIP3_1*, or miR *BNIP3_2*. Arrowheads indicate sunburn-like cells. (**b**) The number of sunburn-like cells per mm was counted and plotted as the means of 10 sections ± SD. (**c–e**) HPEKs were infected with adenovirus expressing miR *neg*, miR *BNIP3_1*, or miR *BNIP3_2*, and irradiated with UVB. (**c**) Cells were stained with anti-EGFP at 8 hours after UVB irradiation. (**d**) The percentage of EGFP-LC3-positive cells with more than five puncta were quantified and are presented as the mean of three independent experiments ± SD. (**e**) Autophagy induction was determined by Cyto-ID staining and quantified by flow cytometry. The data represent the average of three independent experiments ± SD. (**f**) Cells were subjected to western blot analysis at 8 hours after irradiation. The blot shown is representative image of three independent experiments. Graphs indicate relative band intensities as determined by ImageJ software and plotted as the means of three independent experiments. Scale bars = 20 μm. $^{**}P<0.01$.

cytes (Zhao *et al.*, 2013). Because our data indicate that UVB-induced autophagy is mediated by BNIP3 (Figure 6c and d), it is possible that autophagy induced by BNIP3 also plays a role in the maintenance of keratinocytes. Further analysis is required to confirm these results.

UV-induced apoptotic cells appear within 12 hours and are predominately located in the suprabasal differentiated keratinocyte compartment of human skin (Gilchrest *et al.*, 1981). Moreover, differentiated keratinocytes appear to be most sensitive to the UV light that induces p53-dependent apoptosis (Tron *et al.*, 1998). Tron *et al.* (1998) demonstrated that differentiated keratinocytes in p53-null mice exhibited only a small increase in apoptosis after UVB irradiation compared with the increase observed in normal control animals (Tron *et al.*, 1998). Interestingly, because p53 has been reported to directly suppress BNIP3 expression (Feng *et al.*, 2011), BNIP3 might be abundantly upregulated in suprabasal cells in p53-null animals, resulting in the resistance to UVB-induced apoptosis. Indeed, our preliminary study showed that p53 knockdown enhanced UV-induced BNIP3 expression in HPEKs (data not shown). Therefore, BNIP3 expression in suprabasal cells appears to be important for the protection of differentiated keratinocytes from normal environmental stress such as weak UV exposure *in vivo*.

A recent report on a role for autophagy in epidermal barrier formation and function was identified in *atg7*-deficient mice (Rossiter *et al.*, 2013). The authors showed that autophagy was constitutively active in the suprabasal epidermal layers as we report in this study (Figure 2). However, in contradiction to our results, the authors concluded that autophagy was not essential for the barrier function of the skin. This may be because of the presence of an alternative Atg5/Atg7-independent autophagic pathway (Nishida *et al.*, 2009) in the epidermis. This Atg5/Atg7-independent pathway is also independent of LC3, but forms Rab9-positive double-membrane vesicles. Moreover, protein degradation via this pathway is inhibited by 3-MA and is dependent on Beclin 1. Our data demonstrate that: (1) BNIP3 induced the formation of

EGFP-LC3 puncta (Figure 4) and (2) 3-MA significantly diminished the formation of GFP-LC3 puncta and keratinocyte differentiation induced by BNIP3 (Figure 5). These findings suggest that BNIP3 in the epidermis induced both conventional and Atg5/Atg7-independent autophagy. Intriguingly, GFP cleaved from GFP-LC3 also accumulates in the *Atg7*-deficient epidermis (Rossiter *et al.*, 2013), thereby demonstrating the existence of an alternative autophagic pathway (Juenemann and Reits, 2012) in the epidermis. Further investigation will be required to determine whether Beclin 1 and Rab9 are indispensable for the BNIP3-induced autophagy and subsequent differentiation of keratinocytes.

In summary, our data reveal that expression of BNIP3 in granular cells induces autophagy and is involved in the terminal differentiation and maintenance of skin epidermis. Studies on the involvement of autophagy in skin epidermis have attracted considerable attention recently. In addition, increasing evidence suggests the involvement of BNIP3 in the differentiation of several cell types, including oligodendrocytes (Itoh *et al.*, 2003), osteoclasts (Knowles and Athanasou, 2008), and chondrocytes (Zhao *et al.*, 2012); however, the precise role of BNIP3 in this process remains to be investigated. Our study thus provides new insights into the functions of BNIP3 in differentiation and homeostasis.

MATERIALS AND METHODS

Histology and immunofluorescent analysis

Samples and embryos were fixed in 4% paraformaldehyde, embedded in optimal cutting temperature compound, frozen, and sectioned at 10 μm. Sections were then either subjected to hematoxylin and eosin staining or immunohistochemical analysis as previously described (Moriyama *et al.*, 2006). Details are described in Supplementary Materials Online.

Cell culture

HPEKs were purchased from CELLnTEC (Bern, Switzerland) and maintained in CnT-57 (CELLnTEC) culture medium according to the manufacturer's protocol. For induction of differentiation, the medium was changed to CnT-02 (CELLnTEC) at confluent monolayers of HPEKs, followed by adding calcium ions to 1.8 mM. The generation of human skin equivalents was performed using CnT-02-3DP culture medium (CELLnTEC) according to the manufacturer's protocol.

Design of artificial microRNAs and plasmid construction

Oligonucleotides targeting a human BNIP3 sequence compatible for use in cloning into BLOCK-iT Pol II miR RNAi expression vectors (Invitrogen, Carlsbad, CA) were obtained using the online tool BLOCK-iT RNAi Designer. The oligonucleotide sequences used in this study are shown in Supplementary Table S1 online. Cloning procedures were performed following the manufacturer's instructions.

Adenovirus and lentivirus infection

Adenoviruses expressing EGFP, Hes1, BNIP3, and miR *BNIP3* were constructed using the ViraPower adenoviral expression system (Invitrogen) according to the manufacturer's protocol. Lentivirus expressing EGFP-LC3 (from Addgene plasmid 21073, Cambridge, MA) and miR *BNIP3* plasmid was constructed and used to infect keratinocytes as previously described (Moriyama *et al.*, 2012; Moriyama *et al.*, 2013).

RNA extraction, complementary DNA generation, and Q-PCR

Total RNA extraction, complementary DNA generation, and Q-PCR analyses were carried out as previously described (Moriyama *et al.*, 2012). Details of the primers used in these experiments are shown in Supplementary Table S2 online.

Western blot analysis

Western blot analysis was performed as previously described (Moriyama *et al.*, 2012; Moriyama *et al.*, 2013). Details are described in Supplementary Materials Online.

ChIP assay

The ChIP assay was performed using the SimpleChIP Enzymatic Chromatin IP Kit (Magnetic Beads) (Cell Signaling Technology, Danvers, MA) according to the manufacturer's instructions. Hemagglutinin-tagged Hes1 was immunoprecipitated with rabbit polyclonal antibody against hemagglutinin tag (ab9110, Abcam, Cambridge, MA). Immunoprecipitated DNA was analyzed by Q-PCR. Relative quantification using a standard curve method was performed, and the occupancy level for a specific fragment was defined as the ratio of immunoprecipitated DNA over input DNA. Details of the primers used in these experiments are shown in Supplementary Table S2 online.

Flow cytometry analysis

For autophagy detection, Cyto-ID Autophagy detection kit (Enzo Life Sciences, Plymouth Meeting, PA) was used according to the manufacturer's instructions. Details are described in Supplementary Materials Online.

CONFLICT OF INTEREST

The authors state no conflict of interest.

ACKNOWLEDGMENTS

We thank Shogo Nomura, Ayumi Kitagawa, and Riho Ishihama for technical support; Dr Takashi Ueno for helpful discussions; Dr Hiroyuki Miyoshi for the CSII-EF-RfA, pCMV-VSVG-RSV-Rev, and pCAG-HIVg/p plasmids; Dr Tamotsu Yoshimori for pEGFP-LC3 plasmid; and Dr Ryoichiro Kageyama for *Hes1* KO mice. This work was supported by MEXT KAKENHI grant 23791304 to MM. This work was also supported in part by grants from the Ministry of Health, Labor, and Welfare of Japan and a grant from the Program for Promotion of Fundamental Studies in Health Sciences of the National Institute of Biomedical Innovation (NIBIO).

SUPPLEMENTARY MATERIAL

Supplementary material is linked to the online version of the paper at http://www.nature.com/jid

REFERENCES

Aymard E, Barruche V, Naves T *et al.* (2011) Autophagy in human keratinocytes: an early step of the differentiation? *Exp Dermatol* 20:263–8

Bellot G, Garcia-Medina R, Gounon P *et al.* (2009) Hypoxia-induced autophagy is mediated through hypoxia-inducible factor induction of BNIP3 and BNIP3L via their BH3 domains. *Mol Cell Biol* 29:2570–81

Blanpain C, Lowry WE, Pasolli HA *et al.* (2006) Canonical notch signaling functions as a commitment switch in the epidermal lineage. *Genes Dev* 20:3022–35

Chan LL, Shen D, Wilkinson AR *et al.* (2012) A novel image-based cytometry method for autophagy detection in living cells. *Autophagy* 8:1371–82

Chatterjea SM, Resing KA, Old W *et al.* (2011) Optimization of filaggrin expression and processing in cultured rat keratinocytes. *J Dermatol Sci* 61:51–9

Diwan A, Krenz M, Syed FM *et al.* (2007) Inhibition of ischemic cardiomyocyte apoptosis through targeted ablation of Bnip3 restrains postinfarction remodeling in mice. *J Clin Invest* 117:2825–33

Feng X, Liu X, Zhang W *et al.* (2011) p53 directly suppresses BNIP3 expression to protect against hypoxia-induced cell death. *EMBO J* 30: 3397–415

Gilchrest BA, Soter NA, Stoff JS *et al.* (1981) The human sunburn reaction: histologic and biochemical studies. *J Am Acad Dermatol* 5:411–22

Hamacher-Brady A, Brady NR, Logue SE *et al.* (2007) Response to myocardial ischemia/reperfusion injury involves Bnip3 and autophagy. *Cell Death Differ* 14:146–57

Haruna K, Suga Y, Muramatsu S *et al.* (2008) Differentiation-specific expression and localization of an autophagosomal marker protein (LC3) in human epidermal keratinocytes. *J Dermatol Sci* 52:213–5

Ishibashi M, Moriyoshi K, Sasai Y *et al.* (1994) Persistent expression of helix-loop-helix factor HES-1 prevents mammalian neural differentiation in the central nervous system. *EMBO J* 13:1799–805

Itoh T, Itoh A, Pleasure D (2003) Bcl-2-related protein family gene expression during oligodendroglial differentiation. *J Neurochem* 85:1500–12

Juenemann K, Reits EA (2012) Alternative macroautophagic pathways. *Int J Cell Biol* 2012:189794

Kabeya Y, Mizushima N, Ueno T *et al.* (2000) LC3, a mammalian homologue of yeast Apg8p, is localized in autophagosome membranes after processing. *EMBO J* 19:5720–8

Knowles HJ, Athanasou NA (2008) Hypoxia-inducible factor is expressed in giant cell tumour of bone and mediates paracrine effects of hypoxia on monocyte-osteoclast differentiation via induction of VEGF. *J Pathol* 215:56–66

Lippens S, Denecker G, Ovaere P *et al.* (2005) Death penalty for keratinocytes: apoptosis versus cornification. *Cell Death Differ* 12(Suppl 2):1497–508

Mellor HR, Rouschop KM, Wigfield SM *et al.* (2010) Synchronised phosphorylation of BNIP3, Bcl-2 and Bcl-xL in response to microtubule-active drugs is JNK-independent and requires a mitotic kinase. *Biochem Pharmacol* 79:1562–72

Mizushima N, Levine B (2010) Autophagy in mammalian development and differentiation. *Nat Cell Biol* 12:823–30

Mizushima N, Yamamoto A, Matsui M *et al.* (2004) In vivo analysis of autophagy in response to nutrient starvation using transgenic mice expressing a fluorescent autophagosome marker. *Mol Biol Cell* 15:1101–11

Mizushima N, Yoshimori T, Levine B (2010) Methods in mammalian autophagy research. *Cell* 140:313–26

Moriyama H, Moriyama M, Sawaragi K *et al.* (2013) Tightly regulated and homogeneous transgene expression in human adipose-derived mesenchymal stem cells by lentivirus with tet-off system. *PLoS One* 8:e66274

Moriyama M, Durham AD, Moriyama H *et al.* (2008) Multiple roles of Notch signaling in the regulation of epidermal development. *Dev Cell* 14:594–604

Moriyama M, Moriyama H, Ueda A *et al.* (2012) Human adipose tissue-derived multilineage progenitor cells exposed to oxidative stress induce neurite outgrowth in PC12 cells through p38 MAPK signaling. *BMC Cell Biol* 13:21

Moriyama M, Osawa M, Mak SS *et al.* (2006) Notch signaling via Hes1 transcription factor maintains survival of melanoblasts and melanocyte stem cells. *J Cell Biol* 173:333–9

Nishida Y, Arakawa S, Fujitani K *et al.* (2009) Discovery of Atg5/Atg7-independent alternative macroautophagy. *Nature* 461:654–8

Ohtsuka T, Ishibashi M, Gradwohl G *et al.* (1999) Hes1 and Hes5 as notch effectors in mammalian neuronal differentiation. *EMBO J* 18:2196–207

Quinsay MN, Thomas RL, Lee Y *et al.* (2010) Bnip3-mediated mitochondrial autophagy is independent of the mitochondrial permeability transition pore. *Autophagy* 6:855–62

Rossiter H, Konig U, Barresi C *et al.* (2013) Epidermal keratinocytes form a functional skin barrier in the absence of Atg7 dependent autophagy. *J Dermatol Science* 71:67–75

Sassone J, Colciago C, Marchi P *et al.* (2010) Mutant Huntingtin induces activation of the Bcl-2/adenovirus E1B 19-kDa interacting protein (BNip3). *Cell Death Dis* 1:e7

Schweers RL, Zhang J, Randall MS *et al.* (2007) NIX is required for programmed mitochondrial clearance during reticulocyte maturation. *Proc Natl Acad Sci USA* 104:19500–5

Sowter HM, Ratcliffe PJ, Watson P *et al.* (2001) HIF-1-dependent regulation of hypoxic induction of the cell death factors BNIP3 and NIX in human tumors. *Cancer Res* 61:6669–73

Srinivas V, Bohensky J, Shapiro IM (2009) Autophagy: a new phase in the maturation of growth plate chondrocytes is regulated by HIF, mTOR and AMP kinase. *Cells Tissues Organs* 189:88–92

Tron VA, Trotter MJ, Tang L *et al.* (1998) p53-regulated apoptosis is differentiation dependent in ultraviolet B-irradiated mouse keratinocytes. *Am J Pathol* 153:579–85

Vengellur A, LaPres JJ (2004) The role of hypoxia inducible factor 1alpha in cobalt chloride induced cell death in mouse embryonic fibroblasts. *Toxicol Sci* 82:638–46

Walls KC, Ghosh AP, Ballestas ME *et al.* (2009) bcl-2/Adenovirus E1B 19-kd interacting protein 3 (BNIP3) regulates hypoxia-induced neural precursor cell death. *J Neuropathol Exp Neurol* 68:1326–38

Young AR (1987) The sunburn cell. *Photodermatology* 4:127–34

Zhang J, Ney PA (2009) Role of BNIP3 and NIX in cell death, autophagy, and mitophagy. *Cell Death Differ* 16:939–46

Zhao Y, Chen G, Zhang W *et al.* (2012) Autophagy regulates hypoxia-induced osteoclastogenesis through the HIF-1alpha/BNIP3 signaling pathway. *J Cell Physiol* 227:639–48

Zhao Y, Zhang CF, Rossiter H *et al.* (2013) Autophagy is induced by UVA and promotes removal of oxidized phospholipids and protein aggregates in epidermal keratinocytes. *J Invest Dermatol* 133:1629–37

© 2014. Published by The Company of Biologists Ltd | Development (2014) 141, 91-100 doi:10.1242/dev.103168

RESEARCH ARTICLE

STEM CELLS AND REGENERATION

CCAAT/enhancer binding protein-mediated regulation of TGFβ receptor 2 expression determines the hepatoblast fate decision

Kazuo Takayama[1,2,3], Kenji Kawabata[4], Yasuhito Nagamoto[1,2], Mitsuru Inamura[1], Kazuo Ohashi[5], Hiroko Okuno[1], Tomoko Yamaguchi[4], Katsuhisa Tashiro[4], Fuminori Sakurai[1], Takao Hayakawa[6], Teruo Okano[5], Miho Kusada Furue[7,8] and Hiroyuki Mizuguchi[1,2,3,9,*]

ABSTRACT

Human embryonic stem cells (hESCs) and their derivatives are expected to be used in drug discovery, regenerative medicine and the study of human embryogenesis. Because hepatocyte differentiation from hESCs has the potential to recapitulate human liver development *in vivo*, we employed this differentiation method to investigate the molecular mechanisms underlying human hepatocyte differentiation. A previous study has shown that a gradient of transforming growth factor beta (TGFβ) signaling is required to segregate hepatocyte and cholangiocyte lineages from hepatoblasts. Although CCAAT/enhancer binding proteins (c/EBPs) are known to be important transcription factors in liver development, the relationship between TGFβ signaling and c/EBP-mediated transcriptional regulation in the hepatoblast fate decision is not well known. To clarify this relationship, we examined whether c/EBPs could determine the hepatoblast fate decision via regulation of TGFβ receptor 2 (TGFBR2) expression in the hepatoblast-like cells differentiated from hESCs. We found that *TGFBR2* promoter activity was negatively regulated by c/EBPα and positively regulated by c/EBPβ. Moreover, c/EBPα overexpression could promote hepatocyte differentiation by suppressing TGFBR2 expression, whereas c/EBPβ overexpression could promote cholangiocyte differentiation by enhancing TGFBR2 expression. Our findings demonstrated that c/EBPα and c/EBPβ determine the lineage commitment of hepatoblasts by negatively and positively regulating the expression of a common target gene, *TGFBR2*, respectively.

KEY WORDS: Hepatoblasts, c/EBP, CEBP, Human ESCs

INTRODUCTION

Many animal models, such as chick, *Xenopus*, zebrafish and mouse, have been used to investigate the molecular mechanisms of liver development. Because many functions of the key molecules in liver development are conserved in these species, studies on liver development in these animals can be highly informative with respect that in humans. However, some functions of important molecules in liver development might differ between human and other species. Although analysis using genetically modified mice has been successfully performed, it is not of course possible to perform genetic experiments to elucidate molecular mechanisms of liver development in human. Pluripotent stem cells, such as human embryonic stem cells (hESCs), are expected to overcome some of these problems in the study of human embryogenesis, including liver development, because the gene expression profiles of this model are similar to those in normal liver development (Agarwal et al., 2008; DeLaForest et al., 2011).

During liver development, hepatoblasts differentiate into hepatocytes and cholangiocytes. A previous study has shown that a high concentration of transforming growth factor beta (TGFβ) could give rise to cholangiocyte differentiation from hepatoblasts (Clotman et al., 2005). To transmit the TGFβ signaling, TGFβ receptor 2 (TGFBR2) has to be stimulated by TGFβ1, TGFβ2 or TGFβ3 (Kitisin et al., 2007). TGFβ binding to the extracellular domain of TGFBR2 induces a conformational change, resulting in the phosphorylation and activation of TGFBR1. TGFBR1 phosphorylates SMAD2 or SMAD3, which binds to SMAD4, and then the SMAD complexes move into the nucleus and function as transcription factors to express various kinds of differentiation-related genes (Kitisin et al., 2007). Although the function of TGFBR2 in regeneration of the adult liver has been thoroughly examined (Oe et al., 2004), the function of TGFBR2 in the hepatoblast fate decision has not been elucidated.

CCAAT/enhancer binding protein (c/EBP) transcription factors play decisive roles in the differentiation of various cell types, including hepatocytes (Tomizawa et al., 1998; Yamasaki et al., 2006). The analysis of *c/EBPα* (*Cebpa*) knockout mice has shown that many abnormal pseudoglandular structures, which co-express antigens specific for both hepatocytes and cholangiocytes, are present in the liver parenchyma (Tomizawa et al., 1998). These data demonstrated that c/EBPα plays an important role in hepatocyte differentiation. It is also known that the suppression of c/EBPα expression in periportal hepatoblasts stimulates cholangiocyte differentiation (Yamasaki et al., 2006). Although the function of c/EBPα in liver development is well known, the relationship between TGFβ signaling and c/EBPα-mediated transcriptional regulation in the hepatoblast fate decision is poorly understood. c/EBPβ is also known to be an important factor for liver function (Chen et al., 2000), although the function of c/EBPβ in the cell fate decision of hepatoblasts is not well known. c/EBPα and c/EBPβ bind to the same DNA binding site. However, the promoter activity of hepatocyte-specific genes, such as those encoding hepatocyte nuclear factor 6 (HNF6, also known as ONECUT1) and UGT2B1,

[1]Laboratory of Biochemistry and Molecular Biology, Graduate School of Pharmaceutical Sciences, Osaka University, Osaka 565-0871, Japan. [2]Laboratory of Hepatocyte Differentiation, National Institute of Biomedical Innovation, Osaka 567-0085, Japan. [3]iPS Cell-based Research Project on Hepatic Toxicity and Metabolism, Graduate School of Pharmaceutical Sciences, Osaka University, Osaka 565-0871, Japan. [4]Laboratory of Stem Cell Regulation, National Institute of Biomedical Innovation, Osaka 567-0085, Japan. [5]Institute of Advanced Biomedical Engineering and Science, Tokyo Women's Medical University, Tokyo 162-8666, Japan. [6]Pharmaceutical Research and Technology Institute, Kinki University, Osaka 577-8502, Japan. [7]Laboratory of Embryonic Stem Cell Cultures, Department of Disease Bioresources Research, National Institute of Biomedical Innovation, Osaka 567-0085, Japan. [8]Department of Embryonic Stem Cell Research, Field of Stem Cell Research, Institute for Frontier Medical Sciences, Kyoto University, Kyoto 606-8507, Japan. [9]The Center for Advanced Medical Engineering and Informatics, Osaka University, Osaka 565-0871, Japan.

*Author for correspondence (mizuguch@phs.osaka-u.ac.jp)

Received 27 August 2013; Accepted 3 October 2013

Development (2014) doi:10.1242/dev.103168

is positively regulated by c/EBPα but not c/EBPβ (Hansen et al., 1998; Plumb-Rudewiez et al., 2004), suggesting that the functions of c/EBPα and c/EBPβ in the hepatoblast fate decision might be different.

In the present study, we first examined the function of TGFBR2 in the hepatoblast fate decision using hESC-derived hepatoblast-like cells, which have the ability to self-replicate, differentiate into both hepatocyte and cholangiocyte lineages, and repopulate the liver of carbon tetrachloride (CCl_4)-treated immunodeficient mice. *In vitro* gain- and loss-of-function analyses and *in vivo* transplantation analysis were performed. Next, we investigated how TGFBR2 expression is regulated in the hepatoblast fate decision. Finally, we examined whether our findings could be reproduced in delta-like 1 homolog (Dlk1)-positive hepatoblasts obtained from the liver of E13.5 mice. To the best of our knowledge, this study provides the first evidence of c/EBP-mediated regulation of TGFBR2 expression in the human hepatoblast fate decision.

RESULTS

Hepatoblast-like cells are generated from hESCs

First, we investigated whether the hepatoblast-like cells (HBCs), which were differentiated from hESCs as described in supplementary material Fig. S1A, have similar characteristics to human hepatoblasts. We recently found that hESC-derived HBCs could be purified and maintained on human laminin 111 (LN111)-coated dishes (Takayama et al., 2013). The long-term cultured HBC population (HBCs passaged more than three times were used in this study) were nearly homogeneous and expressed human hepatoblast markers such as alpha-fetoprotein (AFP), albumin (ALB), cytokeratin 19 (CK19, also known as KRT19) and EPCAM (Schmelzer et al., 2007) (supplementary material Fig. S1B). In addition, most of the colonies observed on human LN111-coated plates were ALB and CK19 double positive, although a few colonies were ALB single positive, CK19 single positive, or ALB and CK19 double negative (supplementary material Fig. S1C). To examine the hepatocyte differentiation capacity of the HBCs *in vivo*, these cells were transplanted into CCl_4-treated immunodeficient mice. The hepatocyte functionality of the transplanted cells was assessed by measuring secreted human ALB levels in the recipient mice (supplementary material Fig. S1D). Human ALB serum was detected in the mice that were transplanted with the HBCs, but not in the control mice. These results demonstrated that the HBCs generated from hESCs have similar characteristics to human hepatoblasts and would therefore provide a valuable tool to investigate the mechanisms of human liver development. In the present study, HBCs generated from hESCs were used to elucidate the mechanisms of the hepatoblast fate decision.

TGFBR2 expression is decreased in hepatocyte differentiation but increased in cholangiocyte differentiation

The HBCs used in this study have the ability to differentiate into both hepatocyte-like cells [cytochrome P450 3A4 (CYP3A4) positive; Fig. 1B] and cholangiocyte-like cells (CK19 positive; Fig. 1C) (the protocols are described in Fig. 1A). Because the expression pattern of TGFBR2 during differentiation from hepatoblasts is not well known, we examined it in hepatocyte and cholangiocyte differentiation from HBCs. *TGFBR2* was downregulated during hepatocyte differentiation from HBCs (Fig. 1D), but upregulated in cholangiocyte differentiation from HBCs (Fig. 1E). After the HBCs were cultured on Matrigel, the cells were fractionated into three populations according to the level of TGFBR2 expression (TGFBR2-negative, -lo or -hi; Fig. 1F). The HBC-derived TGFBR2-lo cells strongly expressed *αAT* and *CYP3A4* (hepatocyte markers), whereas the HBC-derived TGFBR2-hi cells strongly expressed *SOX9* and integrin β4 (*ITGB4*) (cholangiocyte markers). These data suggest that the TGFBR2 expression level is decreased in hepatic differentiation, but increased in biliary differentiation of the HBCs.

The cell fate decision of HBCs is regulated by TGFβ signals

To examine the function of TGFβ1, β2 and β3 (all of which are ligands of TGFBR2) in the hepatoblast fate decision, HBCs were cultured in medium containing TGFβ1, β2 or β3 (Fig. 2A,B). The expression levels of cholangiocyte marker genes were upregulated by addition of TGFβ1 or TGFβ2, but not TGFβ3 (Fig. 2A), whereas those of hepatocyte markers were downregulated by addition of TGFβ1 or TGFβ2 (Fig. 2B). To ascertain that TGFBR2 is also important in the hepatoblast fate decision, HBCs were cultured in medium containing SB-431542, which inhibits TGFβ signaling (Fig. 2C,D). Hepatocyte marker genes were upregulated by inhibition of TGFβ signaling (Fig. 2C), whereas cholangiocyte markers were downregulated (Fig. 2D). To confirm the function of TGFβ1, β2 and β3 in the hepatoblast fate decision, colony assays of the HBCs were performed in the presence or absence of TGFβ1, β2 or β3 (Fig. 2E). The number of CK19 single-positive colonies was significantly increased in TGFβ1- or β2-treated HBCs. By contrast, the number of ALB and CK19 double-positive colonies was reduced in TGFβ1-, β2- or β3-treated HBCs. These data indicated that TGFβ1 and β2 positively regulate the biliary differentiation of HBCs. Taken together, the findings suggested that TGFBR2 might be a key molecule in the regulation of hepato-bilary lineage segregation.

TGFBR2 plays an important role in the cell fate decision of HBCs

To examine whether TGFBR2 plays an important role in the hepatoblast fate decision, *in vitro* gain- and loss-of-function analysis of TGFBR2 was performed in the HBCs. We used siRNA in knockdown experiments (supplementary material Fig. S2) during HBC differentiation on Matrigel. Whereas TGFBR2-suppressing siRNA (si-TGFBR2) transfection upregulated the expression of hepatocyte markers, it downregulated cholangiocyte markers (Fig. 3A). si-TGFBR2 transfection increased the percentage of asialoglycoprotein receptor 1 (ASGR1)-positive hepatocyte-like cells (Fig. 3B). By contrast, it decreased the percentage of aquaporin 1 (AQP1)-positive cholangiocyte-like cells. These results suggest that TGFBR2 knockdown promotes hepatocyte differentiation, whereas it inhibits cholangiocyte differentiation. Next, we used Ad vector to perform efficient transduction into the HBCs (supplementary material Fig. S3) and ascertained *TGFBR2* gene expression in TGFBR2-expressing Ad vector (Ad-TGFBR2)-transduced cells (supplementary material Fig. S4). Ad-TGFBR2 transduction downregulated the expression of hepatocyte markers, whereas it upregulated cholangiocyte markers (Fig. 3C). Ad-TGFBR2 transduction decreased the percentage of ASGR1-positive hepatocyte-like cells but increased the percentage of AQP1-positive cholangiocyte-like cells (Fig. 3D). These results suggest that TGFBR2 overexpression inhibits hepatocyte differentiation, whereas it promotes cholangiocyte differentiation. Taken together, these results suggest that TGFBR2 plays an important role in deciding the differentiation lineage of HBCs.

To investigate whether hepatoblasts would undergo differentiation in a TGFBR2-associated manner *in vivo*, HBCs transfected/transduced with si-control, si-TGFBR2, Ad-LacZ or Ad-

Development (2014) doi:10.1242/dev.103168

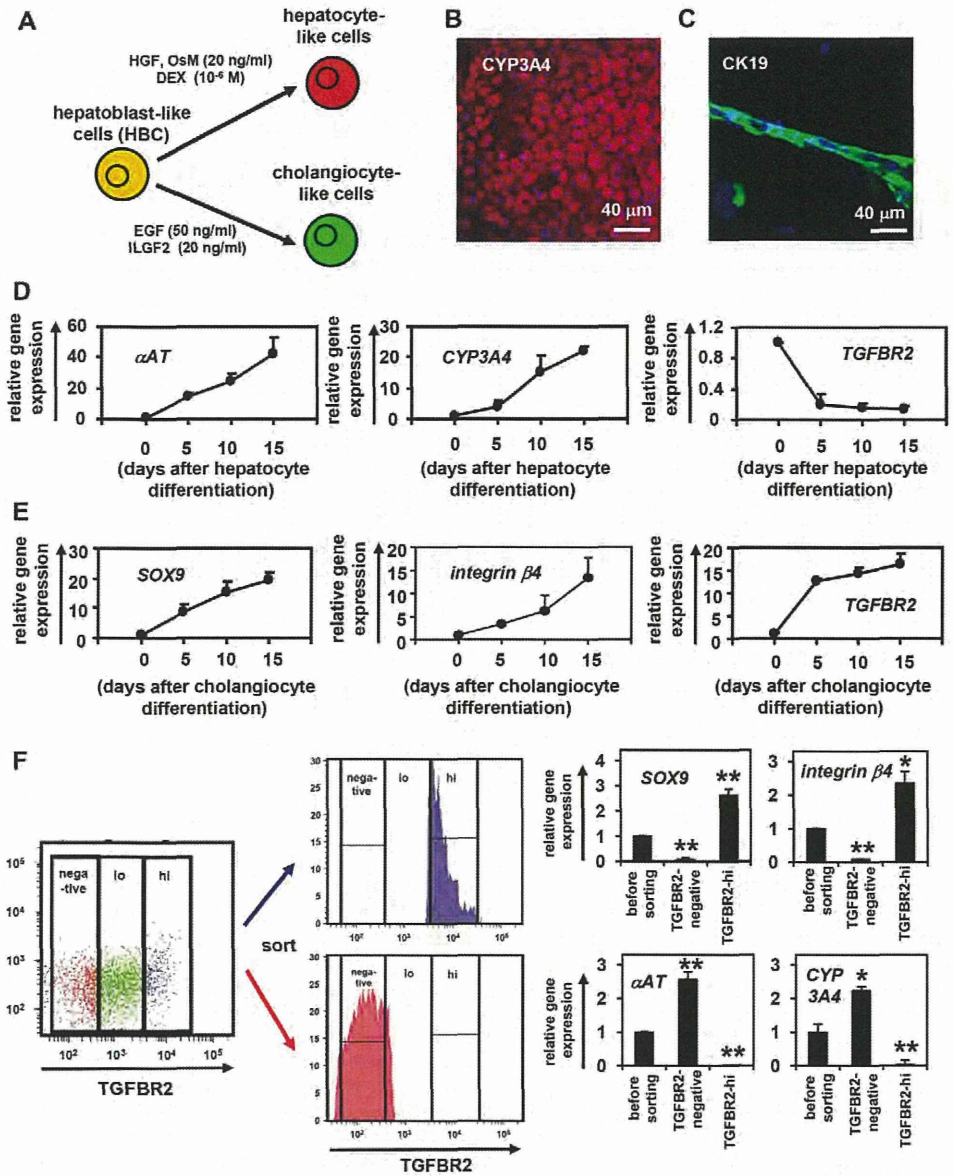

Fig. 1. HBCs can differentiate into both hepatocyte and cholangiocyte lineages. (A) The strategy for hepatocyte and cholangiocyte differentiation from HBCs. (B,C) The HBC-derived hepatocyte-like cells or cholangiocyte-like cells were subjected to immunostaining with anti-CYP3A4 (red, B) or anti-CK19 (green, C) antibodies, respectively. (D,E) Temporal gene expression levels of hepatocyte markers (*αAT* and *CYP3A4*) (D) or cholangiocyte markers (*SOX9* and integrin β4) (E) during hepatocyte or cholangiocyte differentiation as measured by real-time RT-PCR. The temporal gene expression of *TGFBR2* was also examined. The gene expression levels in HBCs were taken as 1.0. (F) HBCs were cultured on Matrigel for 5 days, and then the expression level of TGFBR2 was examined by FACS analysis. TGFBR2-negative, -lo and -hi populations were collected and real-time RT-PCR analysis was performed to measure the expression levels of hepatocyte markers (*αAT* and *CYP3A4*) and cholangiocyte markers (*SOX9* and integrin β4). **P*<0.05, ***P*<0.01 (compared with 'before sorting'). Error bars indicate s.d. Statistical analysis was performed using the unpaired two-tailed Student's *t*-test (*n*=3).

TGFBR2 were transplanted into CCl_4-treated immunodeficient mice (Fig. 3E,F). Although some of the si-control-transfected or Ad-LacZ-transduced HBCs remained as HBCs (HNF4α and CK19 double positive), most of them showed *in vitro* differentiation toward hepatocyte-like cells (HNF4α single positive) (Fig. 3E, top row). By contrast, Ad-TGFBR2-transduced HBCs were predominantly committed to cholangiocyte-like cells (CK19 single positive) and si-TGFBR2-transfected HBCs were predominantly committed to hepatocyte-like cells (HNF4α single positive) (Fig. 3E, bottom row). Ad-TGFBR2 transduction decreased the percentage of HNF4α-positive hepatocyte-like cells, whereas it increased the percentage of CK19-positive cholangiocyte-like cells (supplementary material Fig. S5). The hepatocyte functionality of the *in vivo* differentiated HBCs was assessed by measuring secreted human ALB levels in the recipient mice (Fig. 3F). Mice that were transplanted with Ad-TGFBR2-transduced HBCs showed lower human ALB serum levels than those transplanted with Ad-LacZ-transduced HBCs, and the mice that were transplanted with si-TGFBR2-transfected HBCs showed higher human ALB serum levels than those transplanted with si-control-transfected HBCs. These data suggest that cholangiocyte or hepatocyte differentiation was promoted by TGFBR2 overexpression or knockdown, respectively. Thus, based on these data from *in vitro* and *in vivo* experiments, TGFBR2 plays an important role in deciding the differentiation lineage of HBCs.

TGFBR2 promoter activity and expression are negatively regulated by c/EBPα and positively regulated by c/EBPβ

A previous study has shown that TGFBR2 expression is upregulated in *Hnf6* knockout mice (Clotman et al., 2005), although we confirmed by ChIP assay that HNF6 does not bind to the *TGFBR2* promoter region (data not shown). Because c/EBPα is important in the hepatoblast fate decision (Suzuki et al., 2003), we expected that c/EBPs might directly regulate TGFBR2 expression. The *TGFBR2* promoter region was analyzed to examine whether TGFBR2 expression is regulated by c/EBPs. Some c/EBP binding sites (supplementary material Fig. S6) were predicted by rVista 2.0 (http://rvista.dcode.org/) (Fig. 4A). By performing a ChIP assay, one